Astron. Astrophys. 345, 137–148 (1999)

ASTRONOMY AND ASTROPHYSICS

The contact binary AW Ursae Majoris as a member of a multiple system

T. Pribulla[1], **D. Chochol**[1], **H. Rovithis-Livaniou**[2], **and P. Rovithis**[3]

[1] Astronomical Institute, Slovak Academy of Sciences, SK-059 60 Tatranská Lomnica, Slovakia (pribulla@; chochol@auriga.ta3.sk)
[2] Section of Astrophysics, Department of Physics, University of Athens, GR-157 84 Zografos, Athens, Greece (elivan@atlas.uoa.gr)
[3] Astronomical Institute, The National Observatory of Athens, P.O. Box 20048, GR-11810 Athens, Greece

Received 26 February 1998 / Accepted 22 December 1998

Abstract. New and published UBV photoelectric and spectroscopic observations of AW UMa are analyzed and interpreted by a triple or quadruple-star model. The derived inclination angle i = 78.3°, the photometric mass ratio q = 0.08 as well as all available radial velocities, corrected for the systemic velocity changes, were used to determine the masses of the components of the contact binary as M_1 = (1.79±0.14) $M_\odot$ and M_2 = (0.143±0.011) $M_\odot$. These values set the binary on the ZAMS. Variations in the systemic velocity suggest the existence of a third body on a P_3 = 398 days orbit with eccentricity e_3 = 0.227±0.056. Assuming that the orbits of the contact binary and of the third body are coplanar, its mass is M_3 = (0.85±0.13) $M_\odot$. The long-term orbital period decrease is explained by mass transfer from the more massive to the less massive component accompanied by the angular momentum loss due to mass outflow from the outer Lagrangian point L_2. The period decrease occurred either suddenly (in two period jumps 6200 days apart) or continuously. In the second case, the $(O-C)$ residuals from the parabolic fit can be explained by the light-time effect caused by a fourth body on a P_4 = 6250 days eccentric orbit (e_4 = 0.63±0.24). For the most probable range of inclination of the possible fourth component orbit $60° > i_4 > 40°$, the range of its mass is $0.168\ M_\odot < M_4 < 0.229\ M_\odot$.

Key words: stars: binaries: eclipsing – stars: binaries: spectroscopic – stars: individual: AW UMa

1. Introduction

AW UMa (HD 99946) is a bright (V_{max}=6.84) totally eclipsing A-type W UMa system of spectral type F0-2 (B–V=0.36) with orbital period P = 0.43873 days. The inclination angle of the orbit is $i \approx 79°$. AW UMa is considered as the system with the smallest mass ratio $q \approx 0.075$ among all contact binaries, so it is very interesting from the evolutionary point of view.

Since its discovery by Paczynski (1964), AW UMa was studied photometrically by many authors (for references see Bakos et al., 1991 and Demircan et al., 1992), spectroscopically (Paczynski, 1964; Mochnacki & Doughty, 1972; McLean, 1981; Rensing et al., 1985 and Rucinski, 1992) and polarimetrically (Oschepkov, 1974; Piirola, 1975). A discussion of the most important previous results relevant to our study is given in the appropriate sections.

Send offprint requests to: T. Pribulla

2. Observations and data reduction

2.1. Photoelectric photometry

Most of our photoelectric observations of AW UMa were carried out at the Skalnaté Pleso (SP) and Stará Lesná (SL) observatories of the Astronomical Institute of the Slovak Academy of Sciences. In both cases a single-channel pulse-counting photoelectric photometer installed in the Cassegrain focus of the 0.6 m reflector was used. The integration time was chosen between 6 s and 10 s according to the observational conditions.

Further photoelectric observations were obtained using a two-beam multi-mode photoelectric photometer mounted on the 1.22 m Cassegrain reflector at the Kryonerion Astronomical Station (KAS) of the National Observatory of Athens, Greece.

All SP and SL observations were obtained in the U,B,V passbands except in March 1992, when only the V passband was used. The KAS observations were obtained in the B and V passbands. The stars HD 99832 (V = 7.20, B–V = 0.47, U–B = -0.03) and SAO 62580 (V = 9.47, B–V = 0.73, U–B = -0.24) were used as a comparison and check star respectively. All the observations were corrected for atmospheric extinction and transformed to the standard UBV system. The list of photometric observations is given in Table 1. The KAS observations were used only for determination of the times of minima.

The total number of the SP and SL individual observations exceeded 3000 in each passband. Individual observations of AW UMa are plotted in the phase diagram (Fig. 1) constructed according to ephemerides (2) and (3).

2.2. Optical spectroscopy

Optical spectroscopy in the blue part of the spectrum (360–500 nm) was performed by using the 2 m telescope at the Ondřejov Observatory of the Astronomical Institute of the Academy of Sciences of the Czech Republic from February 29, 1992 to April 7, 1992. Spectra with a reciprocal dispersion 1.75 nm mm^{-1}

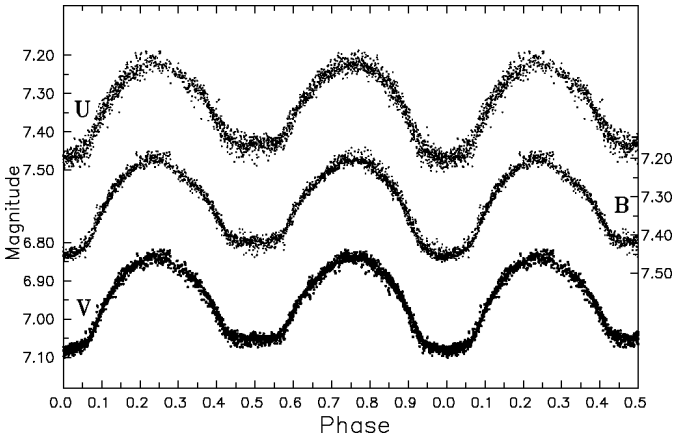

Fig. 1. Photoelectric UBV light-curves of AW UMa

were taken by using a spectrograph mounted at the Coudé focus on Kodak IIaO plates hypersensitized in hydrogen. All spectra were measured with the five-channel microphotometer of the Ondřejov Observatory using the reduction software SPEFO (Horn et al., 1996). The same software package was employed for the reduction of the raw data and analysis of the spectral lines. The spectroscopic observations of AW UMa are listed in Table 2.

At the time of observations of AW UMa two spectra of the standard star 59 Dra (HD180777) were taken. The radial velocity (henceforth RV) measured from the Doppler profiles of hydrogen lines was (-3.8±2.2) km s^{-1} in perfect agreement with the standard velocity -4.0 km s^{-1} given by Duflot et al. (1995). Therefore no zero-point correction was applied to the measured RVs.

Two further spectra were taken with the 1 m telescope of the University of Toledo, U.S.A., on March 3, 1995 and March 1, 1996. The spectra were projected by the high dispersion echelle spectrograph on a 1200x800 CCD chip cooled by liquid nitrogen. The chip was sensitized in the blue part of the spectrum. The spectra comprised nine echelle orders from 547 to 673 nm and were reduced by Dr. K. Gordon. These two spectroscopic observations are listed at the end of Table 2.

Table 1. The journal of photometric observations of AW UMa. Times of observations (middles of the observing runs) are given in JD–2 400 000. Phases were calculated using the ephemerides (2) and (3)

JD$_{hel}$	Phases	Obs.	JD$_{hel}$	Phases	Obs.
45108.41	0.84–0.40	KAS	50099.37	0.11–0.53	SL
45107.49	0.93–0.14	KAS	50139.38	0.30–0.86	SL
46209.43	0.57–0.82	KAS	50141.37	0.84–0.34	SL
46513.48	0.57–0.90	KAS	50161.35	0.38–0.87	SL
46514.40	0.61–0.02	KAS	50180.29	0.54–0.63	SL
46515.40	0.80–0.39	KAS	50421.53	0.41–0.65	SP
46516.33	0.08–0.33	KAS	50423.49	0.87–0.13	SL
48683.45	0.76–0.07	SP	50428.52	0.34–0.77	SL
48684.29	0.67–0.78	SP	50430.47	0.79–0.26	SP
49735.39	0.48–0.04	SP	50461.40	0.28–0.65	SL
49749.52	0.80–0.83	SL	50465.39	0.37–0.65	SL
49778.33	0.36–0.03	SL	50471.50	0.30–0.64	SL
49841.38	0.06–0.51	SL	50486.38	0.21–0.81	SL
49843.31	0.46–0.60	SL	50507.35	0.89–0.17	SL
49862.34	0.82–0.21	SL	50513.46	0.67–0.21	SL
50096.39	0.32–0.70	SL	50799.56	0.96–0.15	SP
50097.51	0.86–0.19	SL	50813.53	0.78–0.03	SP
50098.38	0.85–0.51	SL	50927.41	0.26–0.74	SL

Table 2. The list of spectroscopic observations of AW UMa at the Ondřejov and Toledo observatories. The times of the middles of the exposures are given in JD–2 400 000. The corresponding phases were calculated using the ephemerides (2) and (3). Exposure times are in minutes

JD$_{hel}$	Exp.	Phase	JD$_{hel}$	Exp.	Phase
48682.3545	60	0.259	48683.4733	15	0.809
48682.3948	53	0.351	48683.4851	15	0.836
48682.4247	29	0.419	48683.4969	15	0.863
48682.4518	27	0.481	48683.5094	17	0.892
48682.4705	21	0.524	48683.5261	25	0.930
48682.4900	22	0.568	48683.5455	26	0.974
48682.5025	19	0.597	48720.3840	47	0.940
48682.5164	17	0.628	48720.4264	57	0.037
48682.5309	20	0.661	48720.4812	91	0.162
48683.4469	20	0.749	49779.8038	60	0.703
48683.4615	16	0.782	50143.7758	60	0.313

3. Orbital period changes of AW UMa

3.1. Times of minimum light

Several UBV photometric observations of AW UMa were taken during eclipses. These observations were analyzed using the procedure introduced by Kwee & van Woerden (1956) to determine the times of minima. We have determined the times of 13 primary and 11 secondary minima. Most of them (20) were already published (Pribulla et al., 1997). The heliocentric times of our new 4 minima of AW UMa together with all available photoelectric minima from the literature are listed in Table 3.

Our UBV photometry shows that while the primary minima of AW UMa occur almost simultaneously in all three passbands, the secondary minima in the U passband occur later than in the B and V passbands. The mean delay of the times of secondary minimum in the U passband in comparison with the average times of the secondary minima in the B and V passbands is (96 ± 22) s.

We have used the minima from Table 3 (except last 9) to find the systematic delay of the secondary minima with respect to their expected position in phase 0.5 given by primary minima. The resulting delay ΔT = (54 ± 27) s is even larger than the ΔT = 36 s found by Demircan et al. (1992) and incompatible with an explanation by the internal light-time effect (Liu et al., 1990). Another phenomenon must be responsible for the shift. The large error in its determination suggests that the phenomenon is highly variable.

Table 3. Photoelectric times of minima of AW UMa. Errors (σ) are given in 0.0001 days. Julian dates are $-2\,400\,000$. The last 9 minima were excluded from the study of variations of the minima times

JD_{hel}	σ	Ref.	JD_{hel}	σ	Ref.	JD_{hel}	σ	Ref.	JD_{hel}	σ	Ref.
38045.002		1	44274.7702	8	6	47578.394		16	49862.4120	5	12
38045.8785		1	44277.8396	4	6	47603.4067		16	50096.478	11	12
38046.974		1	44283.7634	4	6	47604.2795		16	50097.5706	7	12
38089.9707		1	44292.5358	2	9	47604.5043		16	50098.44886	0.7	12
38487.6825		2	44294.5093	2	9	47899.5477		16	50139.4693	5	12
38501.7195		2	44320.39578	5.8	10	47903.4955		16	50141.4447	1	12
41333.5178	18	3	44341.453		11	47906.5695		16	50161.40763	4	12
41336.5898	15	3	44343.43098	6.4	10	47983.3462		13	50421.571	5	12
42074.538	10	3	44608.8622	2	6	48011.4263		25	50423.5438	0.4	12
42091.4302	10	3	44664.7993	2	6	48320.5075		16	50428.5918	5	12
42096.4745	17	3	45107.4766	2	12	48332.353		17	50430.5640	4	12
42107.4425	11	3	45108.3531	4	12	48373.3756		16	50461.4979	5	12
42108.5393	12	3	45449.6815	7	13	48644.5117	6	18	50465.44334	5	12
42134.4249	12	3	45460.6545	18	13	48649.5555	8	18	50471.5855	8	12
42140.347	14	3	45773.4679		14	48683.5554	1	12	50486.5023	2	20
42148.4648	7	3	45809.4445		14	49029.4962	14	18	50507.3422	2	20
42151.7539	1	4	45814.4873		14	49032.3486		26	50513.4832	2	20
42152.8495	1	4	45836.6402	21	13	49071.3879		26	50927.4225		20
42153.7287	2	4	46040.6519		14	49074.4635	11	18	42053.91		21
42461.5	10	3	46047.6727		14	49105.3933	8	18	45768.1950	7	22
43125.7334		5	46093.5220		14	49411.4063	8	18	45783.1060	7	22
43580.70074	0.6	4	46100.5407		14	49412.2867	7	18	45795.1712	7	22
43621.722	1	4	46497.5911		14	49412.5015	11	18	45821.2742	7	22
43941.7714	1	6	46499.5648		14	49432.2412		19	46523.6835	38	13
43945.719	1	6	46506.5845		14	49432.4636		18	47930.4720		16
43945.722		7	46514.4813	10	12	49447.1567		19	49426.3409	30	23
43948.7927		7	46515.3586	3	12	49456.1502		19	49444.3212	42	23
43954.7158	2	6	46534.6585	21	13	49458.3488		23			
43966.342		8	47288.398		15	49778.39774	4	12			
43970.7281	5	6	47549.8821		24	49860.4416		27			

References: 1 – Paczynski (1964), 2 – Kalish (1965), 3 – Dworak & Kurpinska (1975), 4 – Woodward et al. (1980), 5 – Eaton (1976), 6 – Hrivnak (1982), 7 – Hart et al. (1979), 8 – Istomin et al. (1980), 9 – Kurpinska-Winiarska (1980), 10 – Mikolajewska & Mikolajewski (1980), 11 – BBSAG 47, 12 – Pribulla et al. (1997), 13 – Bakos et al. (1991), 14 – Heintze et al. (1990), 15 – BBSAG 88, 16 – Demircan et al. (1992), 17 – BBSAG 97, 18 – Müyesseroğlu et al. (1996), 19 – Yim & Jeong (1995), 20 – this paper, 21 – Ferland & McMillan (1976), 22 – Srivastava & Padalia (1986), 23 – Oprescu (1997), 24 -Udalski (Rucinski, 1992), 25 – BAV-M 59, 26 – BAA 81, 27 – BBSAG 109.

3.2. O-C diagram and its explanation

Woodward et al. (1980) found that the orbital period of AW UMa decreases. According to Hrivnak (1982), the observed change can be either sudden or continuous and can be caused by mass transfer from the more massive to the less massive component.

Altogether, we have used 108 minima (given in Table 3) to study the period change. The times of 9 minima deviated too much from the general trend (listed at the end of Table 3) and were therefore excluded from this study.

A linear ephemeris (2) was applied to construct the $(O-C)$ diagram (Fig. 2). The long-term period decrease can be explained as:

1. *Two sudden period changes*. The first jump was detected by Woodward et al. (1980). The second possible jump was detected by the authors (Pribulla et al., 1997). Fitting the data by a broken-line, we derived three linear ephemerides. The ephemeris valid for $E \leq 10495$ is:

$$\begin{aligned}\mathrm{Min\ I} = \mathrm{JD}_{hel}\ &2\,438\,044.7813 &&+ 0.43873231 &&\times E,\\ &\pm 4 &&\pm 5 &&\end{aligned} \quad (1)$$

for $11495 < E \leq 24621$ we have:

$$\begin{aligned}\mathrm{Min\ I} = \mathrm{JD}_{hel}\ &2\,438\,044.8150 &&+ 0.43872910 &&\times E,\\ &\pm 11 &&\pm 6 &&\end{aligned} \quad (2)$$

and finally for $E \geq 24621$ we have:

$$\begin{aligned}\mathrm{Min\ I} = \mathrm{JD}_{hel}\ &2\,438\,044.8923 &&+ 0.43872596 &&\times E.\\ &\pm 80 &&\pm 30 &&\end{aligned} \quad (3)$$

The sum of the squares of residuals for the three linear fits is 0.00031816 d^2. The first sudden period change $\Delta P/P$ = (7.3±0.2) 10^{-6} occurred at JD 2 442 650±105; the second one $\Delta P/P$ = (7.2±0.7) 10^{-6} at JD 2 448 850±115. The time interval between two possible sudden period changes was 6200±150 days (= 17 years).

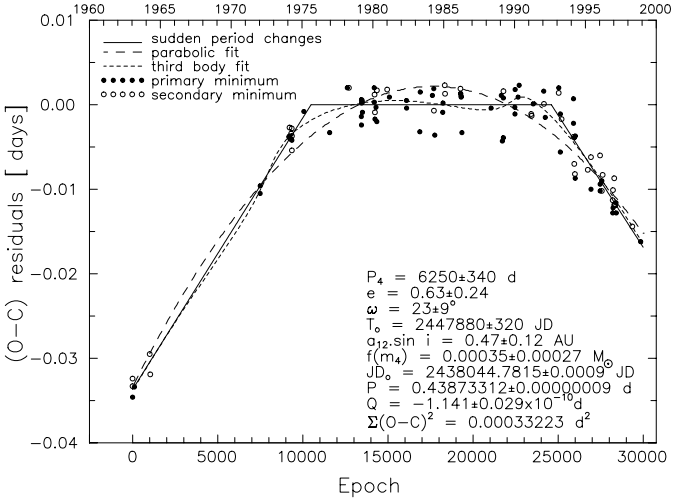

Fig. 2. $(O-C)$ diagram for AW UMa constructed using the ephemeris (2)

2. *Continuous period change*. A parabolic fit provides the following ephemeris:

$$\begin{aligned}\text{Min I} = \text{JD}_{hel}\ 2\,438\,044.7821 &+ 0.43873305 \times E \\ \pm 9 \qquad\quad &\pm 11 \\ &- 1.11\ 10^{-10} \times E^2 \\ &\pm 3\end{aligned} \quad (4)$$

The sum of the squares of residuals is 0.00053518 d^2. The total change of the period is $\Delta P/P$ = (1.42±0.06) 10^{-5}. While the largest residuals from the quadratic fit occurred in 1993-4, the activity of the system reached its maximum four years earlier (see Sect. 5.2). Therefore, the increase of the residuals was not caused only by the activity of the system.

3. *Continuous period change and the light-time effect*. The parabolic fit to the (O-C) data (continuous period change) shows its greatest residuals at the two times cited in case (1) above as possible sudden period changes. These residuals can be reduced by invoking a light-time effect due to an additional body in the system, superimposed on the continuous period change. The times of minima can be computed as follows:

$$\begin{aligned}&\text{Min I} = JD_0 + P \times E + Q \times E^2 + \\ &+ \tfrac{a_{12}\ \sin i}{c} \left[\tfrac{1-e^2}{1+e\cos\nu} \sin(\nu+\omega) + e \sin\omega \right],\end{aligned} \quad (5)$$

where a_{12} sin i is the projected semi-major axis, e is the eccentricity, ω is the longitude of the periastron, ν is the true anomaly. $JD_0 + P \cdot E + Q \cdot E^2$ is the quadratic ephemeris of the minima in an eclipsing binary and c is the velocity of the light.

A preliminary period of the light-time effect was found by Fourier period analysis of residuals from the quadratic fit as P_4 = 6500±1200 days. The parameters of the fit obtained by simultaneous fitting of the light-time effect and parabolic ephemeris obtained by the differential corrections method are given in Fig. 2. The sum of squares of residuals is 0.00033223 d^2. The period of the body P_4 = 6250±340 nearly coincides with the time interval between possible jumps (case 1). The body responsible for such a light-time effect would cause the systemic velocity to change with an amplitude of 0.9 km s^{-1}, which is much smaller than the observed one (see Sect. 7).

Table 4. Fourier coefficients of the mean light-curves

	V	B	U
A_0	0.8956±0.0004	0.8880±0.0004	0.8916±0.0005
A_1	−0.0020±0.0006	−0.0031±0.0006	−0.0032±0.0007
A_2	−0.0994±0.0006	−0.0986±0.0006	−0.0987±0.0008
A_3	−0.0078±0.0006	−0.0094±0.0006	−0.0106±0.0008
A_4	−0.0036±0.0006	−0.0047±0.0006	−0.0058±0.0008
B_1	−0.0001±0.0006	0.0004±0.0006	0.0010±0.0008
B_2	−0.0004±0.0006	0.0010±0.0006	0.0010±0.0007
B_3	−0.0003±0.0006	0.0000±0.0006	−0.0007±0.0008
B_4	0.0000±0.0006	−0.0001±0.0006	−0.0015±0.0007

To summarize, the data can be interpreted as two sudden period changes or as one continuous period change (quadratic fit). In the latter case, the residuals show a systematic effect which can be interpreted as the light-time effect due to another body. Although the sum of the residuals is smaller in the first case, the resulting fits for both cases differ only slightly (see Fig. 2). The present data are not sufficient to decide which interpretation is correct.

4. Photometric light-curves and their analysis

4.1. Normal points and Fourier analysis of the mean light-curves

All our individual observations of AW UMa were used to construct 250 normal points of the mean light-curve (henceforth LC) in each passband. Each normal point is the mean value of brightness in ranges of 0.004 of the orbital phase and was calculated using 12 individual observations in average. The numbers of individual points coming into one normal point were used as weights. The mean UBV LCs were used for a Fourier analysis. The resulting Fourier coefficients are given in Table 4.

Due to the fact that AW UMa is an A-type contact binary with a slightly hotter (and more massive) primary, the coefficient A_1 is negative in all passbands. As $T_1 \approx T_2$, the half amplitude of the light changes is nearly the same in all passbands (as indicated by A_2). The coefficient B_1, reflecting the O'Connell effect, has its largest absolute value in U. As it is positive, the maximum I is somewhat brighter. There is no significant O'Connell effect in B and V. Comparison of the absolute values of B_i coefficients shows that all types of asymmetries of the LC increase from V to U.

The rough estimate of the main photometric elements from Fourier coefficients fails in systems with $q \leq 0.2$ (Rucinski, 1973). As this is the case of AW UMa, we have not made this estimate.

4.2. Photometric elements

The UBV LCs were analyzed using the synthetic LCs and the differential corrections code developed by Wilson & Devinney (1971) (W&D). Particular numbers of individual points coming into one normal point were used as weights. Mode 3 of the W&D code was employed assuming synchronous rotation and blackbody radiation. We have assumed T_1 = 7175 K and solved all LCs simultaneously. The input parameters were taken from Hrivnak (1982). The differential corrections code was run until the output corrections were smaller than the probable errors σ of the elements.

The LC analysis of contact systems is complicated by strong correlations between some elements (see Wilson & Biermann, 1976). Moreover, a LC solution is usually insensitive to bolometric albedo and, to a smaller extent to gravity and limb darkening. Our solution of the LC of AW UMa was aimed at detection of the third light which could be ascribed to a possible third component (see Sect. 7). In previous studies (Hrivnak, 1982; Mochnacki & Doughty, 1972; Wilson & Devinney, 1973) the third light was set to zero. In solution 1 (see Table 5) we have fixed several parameters ($g_1 = g_2, A_1 = A_2, T_1$) from the study of Hrivnak (1982). The limb darkening coefficients ($x_1 = x_2$) were taken from Grygar et al. (1972). The range of photometric and spectroscopic ratios found in previous studies varies from 0.0716 (Wilson & Devinney) to 0.08 (Mauder, 1972) and from 0.07 (McLean, 1981) to 0.086 (this paper) respectively. Due to problems with convergence of solution 1, we have held the mass ratio fixed at values from 0.071 to 0.082 (with the step of 0.001). For $q \leq 0.077$ the third light was negative in the V filter, so these unphysical solutions were omitted in further discussion. For $q \geq 0.078$ the positive third light in all passbands increased with q. The weighted sum of squares reached a minimum for $q = 0.078$, but varied in other solutions only within a few%. The solution with fixed L_3 = 0 led to q = 0.071.

We have also tried to adjust all parameters (except T_1). Although the fit of the LC is better, the resulting values of $A_1 = A_2, g_1 = g_2, x_1 = x_2$ differ from the theoretical values. On the other hand, the derived value of $q_{ph} = 0.080$ is closer to the spectroscopic mass ratio $q_{sp} = 0.086 \pm 0.006$ found from the Toledo spectra (see Sect. 6).

The normal points as well as the LC from solution 2 are depicted in Fig. 3. Although the fits of the B and V LCs are quite good, there is a significant difference between the fit and the mean U LC around the maximum II. Furthemore, there are difficulties with exact fitting of the minima. A non-uniform distribution of the temperature on the surface of the components, caused by spot(s) as well as the presence of circumstellar matter can be responsible for these differences. Since Maceroni & van't Veer (1993) demonstrated that the determination of the position of spots is not unique, we have not tried to improve the solutions by spots.

The most interesting result of our analysis is the detection of the third light, which increases from V to U (solution 2). It is hard to know if the derived values of L_3 tell us something physical about the system, or if they are parameters which adjusted to fit some of the complications in the LCs. In Sect. 7 we derived the mass of the third body as M_3 = (0.85±0.13) $M_\odot$. If it is a main-sequence star, its luminosity has to be L_3 = 0.076±0.040 L_1 ($L \sim M^{3.45}$, Allen, 1976), with the maximum of energy distribution in V, which is not observed. The derived energy distribution is more compatible with the presence of a white dwarf in the system and/or of a hot polar region (not being eclipsed) on the contact binary.

In further calculations we have adopted $i = 78.3°$ and $q = 0.08$ from our LC solutions.

Table 5. Photometric elements of AW UMa and their probable errors σ. Parameters not adjusted in the first solution were denoted by a superscript "a".

Element		1	σ	2	σ
i [°]		79.1	0.1	78.3	0.1
q		0.078^a	–	0.0803	0.0005
fill–out		0.671	0.016	0.846	0.023
g_1=g_2		0.450^a		0.120	0.067
A_1=A_2		1.0^a	–	0.7	0.4
T_2 [K]		6960	9	7022	12
$\frac{L_1}{L_1+L_2}$	U	0.9123	0.0005	0.9033	0.0018
	B	0.9099	0.0005	0.9014	0.0016
	V	0.9078	0.0005	0.8998	0.0014
L_3	U	0.0841	0.0052	0.0643	0.0186
	B	0.0853	0.0049	0.0383	0.0159
	V	0.0208	0.0050	0.0052	0.0137
x_1=x_2	U	0.700^a	–	0.676	0.028
	B	0.770^a	–	0.601	0.023
	V	0.580^a	–	0.484	0.020
$\sum w(O-C)^2$	U	0.0045	–	0.0042	–
	B	0.0032	–	0.0028	–
	V	0.0033	–	0.0029	–

5. Variations of AW UMa light-curves

The LCs variations are quite common in W UMa systems. Differences between the LCs obtained at different epochs were also detected in AW UMa.

Mauder (1972) pointed out that the LC variations in W UMa systems can occur in the course of a single night. To check this possibility, we have estimated the standard deviations of counts for AW UMa and for the comparison star by fitting them with trigonometric polynomials. This computation was done in each passband separately for all nights in which our observations were taken. As the brightness of AW UMa and the comparison star were nearly the same, we can expect the same scatter of individual observations. The scatter of U and B observations of AW UMa was markedly larger than that of the comparison star only in May, 1995. Except for this period, AW UMa was in a non-active stage during our observations.

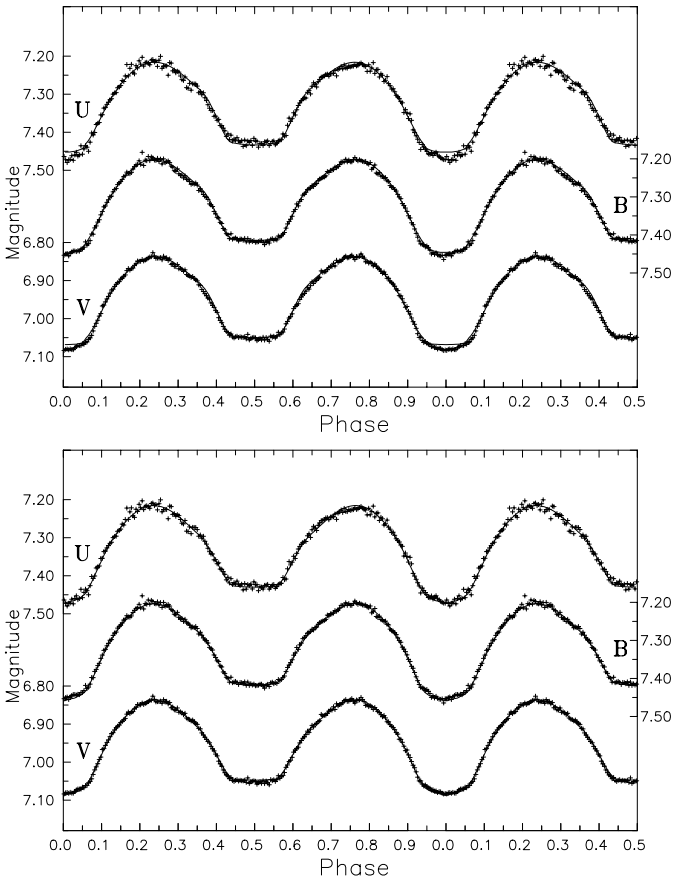

Fig. 3. Mean light-curves and the best fits. Solution (1) *top*, solution (2) *bottom*

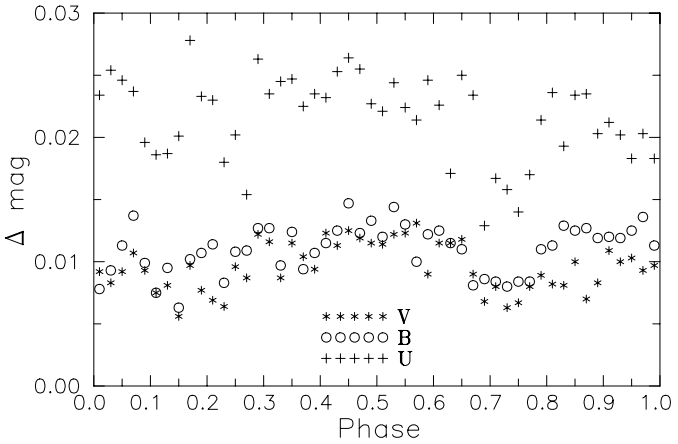

Fig. 4. Phase dependence of the scatter of observations in UBV passbands. The phases were calculated using the ephemerides (2) and (3)

To find a phase dependence of the scatter we have divided the orbital period into 50 intervals and determined the standard deviation of the individual observations in each interval and passband taking into account all the observations. As shown in Fig. 4, the largest scatter occurred around the secondary minimum (explained by the long-term LC variations or possible mid-eclipse brightening), and the smallest scatter around the maximum II.

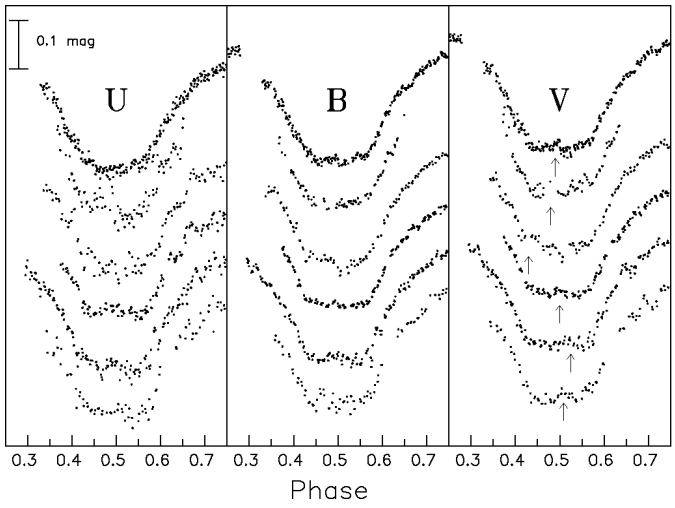

Fig. 5. "Mid-eclipse brightening" (indicated by arrows). The dates of observations (upwardly) Mar 1, 1995; Feb 25, 1996; Mar 18, 1996; Dec 10, 1996; Jan 16, 1997 and Feb 6, 1997

5.1. Mid-eclipse brightening?

A very interesting feature of the LC is the variability in the secondary minimum, firstly reported in AW UMa by Kudzej (1987) as mid-eclipse brightening. As an explanation, he proposed the refraction of the radiation of the secondary in the atmosphere of the primary. He argued that the effect is measurable only in the presence of a strong magnetic field. IUE spectroscopy of AW UMa has shown that its magnetic activity is negligible (Rucinski et al., 1984).

The mid-eclipse brightening does not occur at every secondary minimum. Moreover, its position and relative height is variable (Fig. 5). The average amplitude of the brightening, best visible in the V light (due to the lowest scatter of observations), is about 0.02 mag. We have found a mid-eclipse brightening also in published LCs taken in February 1963 (Paczynski, 1964) and in March-April 1985 (Bakos et al., 1991). The mid-eclipse brightening is also visible in Fig. 1.

5.2. Long-term changes of the LC and photometric elements

Intrinsic variations of the AW UMa LC were observed and discussed by Hrivnak (1982), Derman et al. (1990) and Bakos et al. (1991). Hrivnak (1982) observed and separately analyzed two types of LC: faint and bright. He found that the faint LC corresponds to a larger fill-out factor of the system and to a lower temperature of the secondary component. To explain the photometric variability of the system, the author proposed two alternative models: (i) variations in temperature and size of the secondary component and intermittent outflow of matter from L_2 (ii) variable hot spot on the back of the secondary component. The most pronounced changes of the LC and colour indices, as large as 0.15 mag, were observed in 1989–90 by Derman et al. (1990). They explained them by fast mass transfer and variable spots.

Table 6. Radial velocities of the primary component in km s^{-1}. The phases were calculated using the ephemeris (2)

Phase	All lines RV	σ	H_γ RV	Phase	All lines RV	σ	H_γ RV
0.037	−42	7	−31	0.661	−14	6	−13
0.162	−50	9	−54	0.749	−2	9	0
0.259	−51	7	−48	0.782	−6	5	4
0.351	−46	5	−45	0.809	−11	4	−6
0.419	−33	6	−36	0.836	1	8	−9
0.481	−29	4	−23	0.863	−3	7	−14
0.524	−32	8	−24	0.892	−7	3	−2
0.568	−22	6	−10	0.930	−20	6	−18
0.597	−19	5	−12	0.974	−14	4	−20
0.628	−15	7	−7	0.940	−7	9	−17

Bakos et al. (1991) observed four types of LCs: shallow, deep, intermediate and extraordinary. They differ mainly in the depth of the primary minimum. Transitions from shallow to deep LC lasted a few days. The authors explained LC variations by a non-uniformly distributed matter around the primary component, without attempt at determining the photometric elements. We have analyzed their LCs by the W&D code to find the photometric elements most affected by the LC changes. We have fixed the geometrical elements determined in Sect. 4 (q = 0.08, i = 78.3°). While we have got T_2 = 6970±30 K and a fill-out factor f = 0.95±0.01 for the shallow LC, we were not able to obtain a physical solution for the deep LC (the differential corrections did not converge). It is impossible to explain the large dip of the brightness during primary minimum in the deep LC solely by changes of the photometric parameters of the system. The best explanation provides the stream of matter escaping from L_2, when the system fills up the outer critical surface.

In this paper, we refer to the epochs of large variations of the LC as active stages.

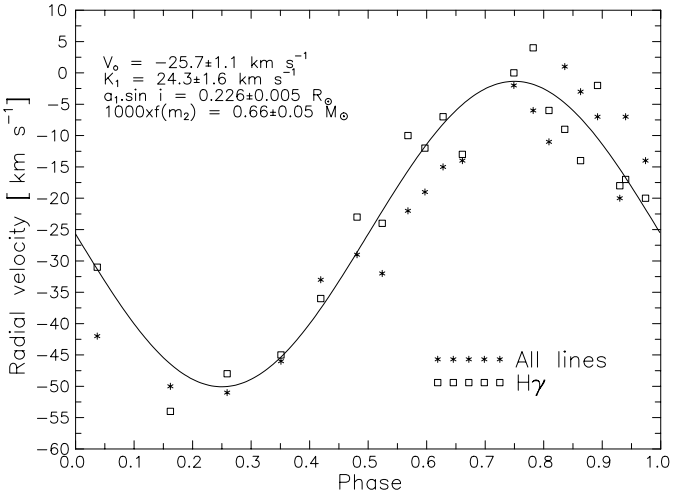

Fig. 6. Radial velocities of the primary component of AW UMa, the fit for H_γ line and corresponding elements of the spectroscopic orbit

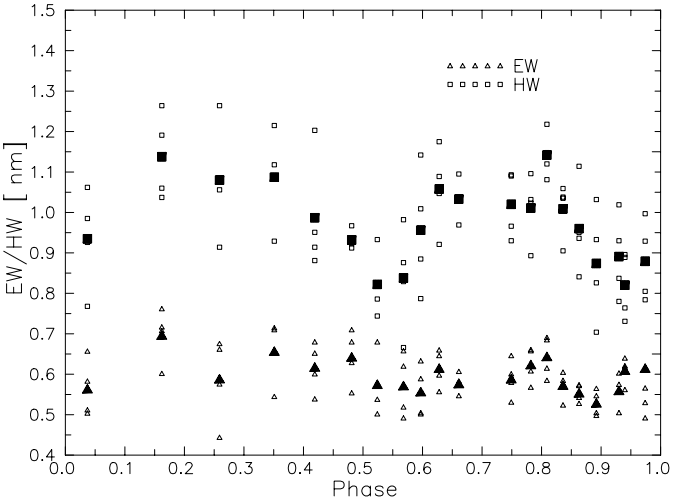

Fig. 7. EWs and HWs of hydrogen lines. Large symbols denote average values for the particular spectrum

6. Analysis of spectroscopic observations

AW UMa is a F0-2 star, thus it has a pure absorption spectrum dominated by the lines of neutral hydrogen and ionized calcium (H and K line). Metallic lines are quite weak. The secondary component lines, very weak because of the low mass ratio, can be detected only near quadratures. The very rapid orbital motion, rather long exposure times and the lower signal-to-noise ratio caused by the use of photographic plates prevented us from measuring the secondary component lines on the spectra from the Ondřejov observatory, but they were well resolved and measured on the two CCD spectra from Toledo.

Our spectroscopic analysis is mainly based on 20 spectra taken at the Ondřejov observatory in 1992. We have used the H_β, H_γ, H_δ and H_8–H_{14} lines to measure the radial velocities (RV) of the primary component. The blend of H_ε and Ca II H lines was omitted from the analysis. The RVs were measured by the oscilloscopic method using the software SPEFO. The results are given in Table 6 and Fig. 6.

H_β line is on the edge of the spectral sensitivity of the Kodak IIaO plate. Since the intensity of hydrogen lines decreases towards the Balmer jump, the most suitable line for RV measurements is H_γ. The elements of the spectroscopic orbit computed from the measured RVs of this line are given in Fig. 6. It is necessary to note that the deviations from the average RV increase from H_γ to H_{14}. In both solutions, a zero eccentricity and a period P = 0.43873 days were fixed.

We have measured the halfwidth (HW) and equivalent width (EW) of the H_β, H_γ, H_δ and H_8 lines (Fig. 7). The HWs of the lines depend on phase in the same manner as shown by Paczynski (1964). They exhibit two maxima and minima as expected for a contact binary. We have found HWs around the maximum I to be slightly larger than around maximum II. The phase dependence of EWs is different. They change throughout the orbital phase only a little, but the minimum around the phase 0.9 seems to be real. The large EW in phase 0.169 can be partly influenced by the long exposure time (91 min.) of the spectrum.

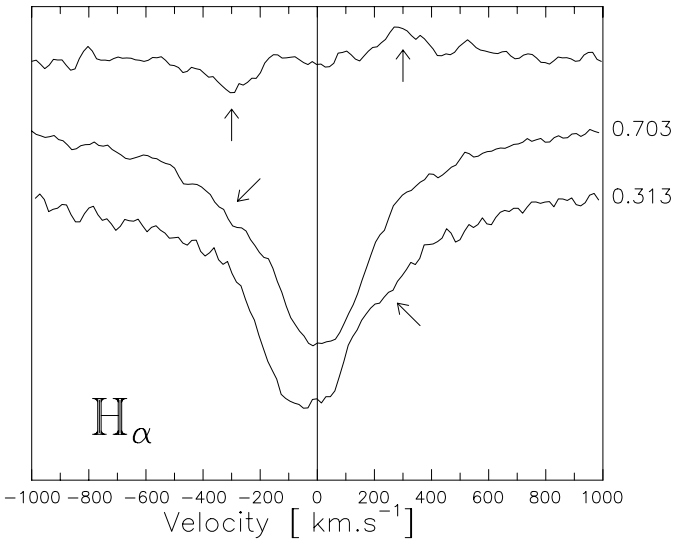

Fig. 8. H_α profiles taken in orbital phases 0.313 and 0.703. Subtraction of the profiles clearly shows the presence of the secondary component

Table 7. New determination of the spectroscopic elements of AW UMa from published data

	Original		New	
Author	$V_{0,b}$	K_1	$V_{0,b}$	K_1
	[km s^{-1}]		[km s^{-1}]	
Paczynski (1964)	−1.3	28	−1.3	27.6
	±2	±3	±2.2	±2.9
McLean (1981)	−17	29	−22.6	25.8
	±7	±8	±4.3	±5.3
Rensing et al. (1985)	−0.8	22.2	−0.8	22.2
	±1.6	±0.9	±0.6	±0.8
Rucinski (1992)*	−7.1	–	−7.0	28.8
	±1.2	–	±1.1	±1.6
Rucinski (1992)**	−8.9	–	−8.8	33.3
	±1.6	–	±1.2	±1.5
this paper	–	–	−25.7	24.3
	–	–	±1.1	±1.6

* 1988 observations, ** 1989 observations

The two spectra from Toledo with high S/N ratio were also used for the RV measurements. The only usable line is H_α. We have determined RV = (11±2) km s^{-1} and RV = (-36±2) km s^{-1} for the spectra taken on March 3, 1995 (phase 0.703) and March 1, 1996 (phase 0.313), respectively. The corresponding systemic velocities calculated using the difference between measured and expected RV (assuming K_1 = (25.3±0.6) km s^{-1}, see Sect. 7) of the primary component in phases 0.703 and 0.313 were (-13.2±2.1) km s^{-1} and (-12.6±2.1) km s^{-1}, respectively. The spectra were taken near quadratures, so their simple subtraction (after correction for RV of the primary component) enabled us to measure RVs of the secondary component in both phases simultaneously (Fig. 8). The mass ratio calculated from the ratio of the RVs of the primary and secondary component corrected for the systemic velocity shift is q = 0.084±0.006 and q = 0.088±0.006 for the first and second spectrum, respectively.

7. Masses of the contact binary and the third component in the system

The systemic velocity of AW UMa determined from the Ondřejov spectra does not agree with the values found from the Toledo spectra and there are also differences in its determination among other authors. We will go on to show briefly the evidence for a third body, and hereafter $V_{0,b}$ and $V_{0,t}$ designate the velocities of the mass centres of the binary and triple system, respectively.

McLean (see Rensing et al., 1985) changed its original value $V_{0,b}$ =(-17±7) km s^{-1} (McLean, 1981) to $V_{0,b}$ = (-9±7) km s^{-1} (McLean, 1983). Rucinski (1992) excluded four determinations of the RV to reduce the discrepancy in systemic velocity with previous determinations.

We reanalyzed all the original data using the ephemerides (1)-(3). The correction of the phases for the McLean's (1981) data was as large as 10% of the orbital period. The original and the new values of systemic velocities $V_{0,b}$ and amplitudes of the RV curve are given in Table 7.

To find out whether the differences in systemic velocity of binary are real or caused only by the scatter of observations, we have applied zero-point shifts to all available RVs of AW UMa. The individual RVs of the primary component before and after the correction for $V_{0,b}$ are shown in Fig. 9. The sum of squares of residuals for the original data (70287 km^2 s^{-2}) is more than three times larger than that for the corrected data (19642 km^2 s^{-2}).

This result as well as the $V_{0,b}$ study indicate that the variations in $V_{0,b}$ are real. We interpret them as evidence for the presence of the third component in the system. It is interesting to note, however, that when previous investigators observed the system over two consecutive seasons, they measured the same $V_{0,b}$ each season (Rensing et al. 1985, Rucinski 1992). A similar effect is seen in our two Toledo observations. One might alternatively conclude that the variations in $V_{0,b}$ are due to systematic effects between different telescopes rather than to a third body. However, systematic effects seem to be ruled out by the use of radial velocity standard stars (except for our Toledo observations). The agreement in the values of $V_{0,b}$ in observations of successive seasons is due to the fact that the period of the third body happens to be comparable to the one-year observing interval.

7.1. New spectroscopic elements of the contact binary

Altogether we have 149 determinations of the RV at our disposal. These data, corrected for particular $V_{0,b}$ and weighted to account for the different qualities of the spectroscopic observations, were used to obtain a more accurate spectroscopic orbit of the contact system. The new spectroscopic elements are given in Fig. 9 (bottom). Adopting a photometric mass ratio q = 0.08 and an inclination angle i = 78.3°, we derive the masses of the

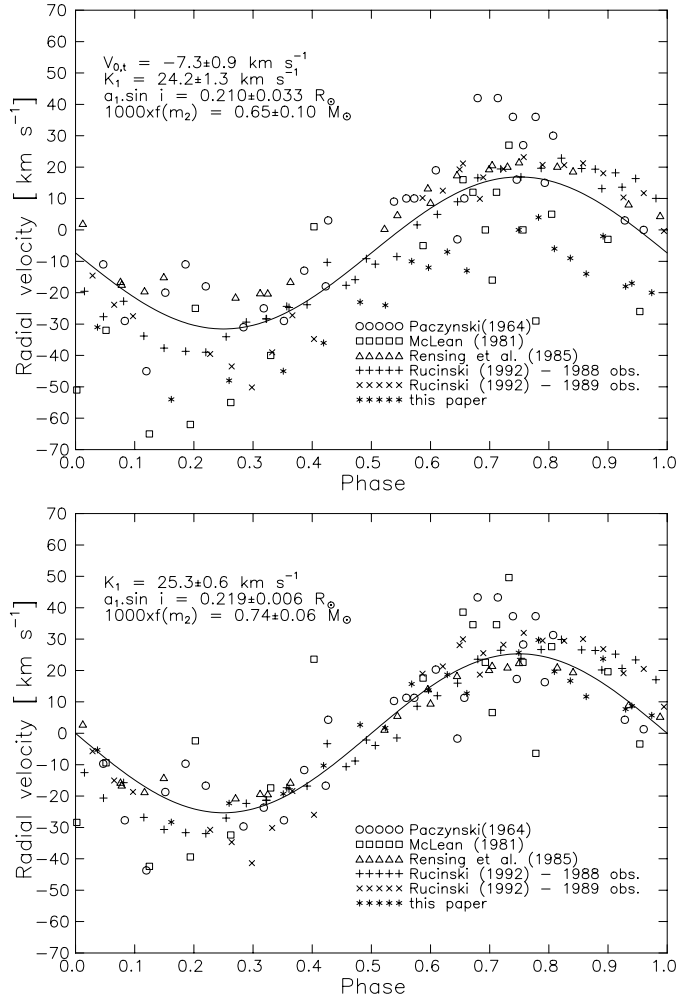

Fig. 9. Radial velocities of the primary component of AW UMa before (*top*) and after (*bottom*) correction for $V_{0,b}$

components of the contact binary as M_1 = (1.79±0.14) M$_\odot$ and M_2 = (0.143±0.011) M$_\odot$.

One must be aware, however, that the set of RVs of the primary component is quite inhomogeneous due to the different methods used for finding RVs: cross-correlation (McLean, 1981), synthetised profile (Rensing et al., 1985), broadening function with model profiles (Rucinski, 1992) and line measurements (Paczynski, 1964; this paper). Since some methods do not take into account the secondary component, the RV of the primary is underestimated because of the line profile blending with the secondary (Paczynski,1964; Rensing et al., 1985 and this paper). It is important to note that proximity effects in contact binaries tend to make the light center closer to the companion star than is the center of mass and thus tends to underestimate K_1 (Hrivnak, 1988). Rensing et al. (1985), however, state that the distortion effects are not important for AW UMa.

7.2. Parameters of the third component

The third component in the system causes not only changes in the systemic velocity, but also a light-time effect, which can be found in the residuals from the broken-line fit (two sudden period changes). Since the residuals for the third case nearly coincide, henceforth we will assume the first case of period change.

We have tried to find a solution taking into account both effects simultaneously. The main problem is the large number of "free" parameters. Some of them, however, are not independent. If we compare the formulae for the light-time effect (Irwin, 1959):

$$\Delta t = \frac{a_{12}\sin i}{c}\left[\frac{1-e^2}{1+e\cos\nu}\sin(\nu+\omega)+e\sin\omega\right] \quad (6)$$

and for $V_{0,b}$ (e.g. Binnendijk, 1960):

$$V_{0,b} = V_{0,t} + \frac{2\pi a_{12}\sin i}{P\sqrt{1-e^2}}(e\cos\omega+\cos(\nu+\omega)), \quad (7)$$

we get the amplitudes as follows:

$$A_{light} = \frac{a_{12}\sin i}{c}, A_{RV} = \frac{2\pi a_{12}\sin i}{P\sqrt{1-e^2}}. \quad (8)$$

Excluding of $a_{12}\sin i$ from the above equations yields:

$$P = \frac{2\pi c}{\sqrt{1-e^2}}\frac{A_{light}}{A_{RV}}. \quad (9)$$

For A_{light} and P in days and A_{RV} in km s^{-1} we obtain:

$$P = \frac{1.8836\ 10^6}{\sqrt{1-e^2}}\frac{A_{light}}{A_{RV}}. \quad (10)$$

Using the equation (10) we constrained the range of possible periods of the third body. Thereafter we have found the value of period of the third body by a period analysis of the systemic velocity and light-time curves separately.

The amplitude of $(O-C)_2$ residuals is ≈ 0.0025 days (σ = 0.0017). The amplitude of the systemic velocity variations $V_{0,b}$ is A_{RV} = 12.5 km s^{-1}. It is easy to find that for a reasonable range of eccentricities $0 < e < 0.9$ the orbital period of the third component is in the range 380–880 days. The most significant periods in this range found by the Fourier analysis in systemic velocities $V_{0,b}$ and $(O-C)_2$ residuals from the broken-line fit are 398±5 days and 402±8 days, respectively. The $(O-C)_3'$ residuals from the possible fourth body fit provide 407±8 days periodicity. The period of 400 days was used as the initial value for our differential corrections code, which solves the light-time effect and systemic velocity curve simultaneously. In our solution we have put weight 10 to the set of systemic velocities $V_{0,b}$ and 1 to the set of $(O-C)_2$ data since systemic velocities were usually determined from many RV measurements. Individual systemic velocities were weighted according to their errors (for the fitting we have also used two estimates of $V_{0,b}$ from two Toledo spectra).

We have found that the best fit for the third component corresponds to an orbital period P_3 = 398 days (Fig. 10). The systemic velocity of the triple system is $V_{0,t} \approx$ -15.6 km s^{-1}. It is important to note that Rensing et al. (1985) and Rucinski (1992) observed AW UMa in two intervals approximately 400 and 380

days apart, respectively. This is the reason why they did not find a change of the systemic velocity in their spectroscopic data.

Although the $V_{0,b}$ fit is perfect, the corresponding fit in $(O-C)_2$ diagram, due to the large scatter of data, is not as good. Hrivnak (1982) estimated that the asymmetry of the LC can cause deviations as large as 0.004 days while the amplitude of the light-time effect caused by the presence of the third body is only about 0.00258 days.

The minimum mass of the third component determined from the mass function and the mass of the contact system is M_3 = (0.85±0.13) $M_\odot$.

The energy distribution of the third light suggests that the third component is a white dwarf (see Sect. 4.2). Therefore it is not expected to be seen on our high dispersion spectra from Toledo. Nevertheless, due to the problems with the exact photometric solution, we cannot exclude the possibility that the third component is a main sequence star. In such a case the ratio of its luminosity and that of the primary component is 0.076±0.040. Thus it could be detected on high-dispersion spectra. The expected range of its RVs is -16 to 58 km s^{-1}, so the lines of the third component are always located in the Doppler core of the primary component lines. This complicates the spectroscopic detection of the third component. This component can cause not only a shift of the line center (affecting $V_{0,b}$ and K_1) but also the narrowing of the composite line profile. Indeed Mochnacki & Doughty (1972) found the observed profile of H_γ line to be narrower than the synthetic one.

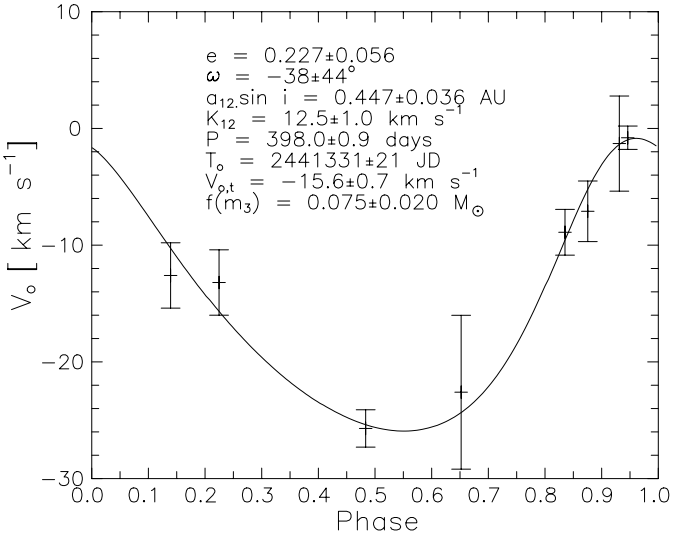

Fig. 10. Systemic velocities and their best fit for a period of 398 days

8. Discussion and conclusion

8.1. Contact binary

The peculiar observational effects (complications) which have to be taken into account to make a detailed model of the system are as follows:

- The long-term period decrease of the orbital period;
- The secondary minimum in the U light occurring (96±22) s later than in the B and V lights;
- The delay of the secondary minima ΔT = (54±27) s;
- The larger variations of the LC around maximum I than around maximum II. The maximum I in the U light is about 0.01 mag brighter than the maximum II;
- The lowest scatter of observations is around maximum II;
- During the active stages the relative brightness of maxima varies. In some LCs the maximum I is suppressed, so the maximum II becomes brighter;
- Asymmetries of the LC increasing from the V to U light;
- The presence of the third light in the photometric solutions of the UBV LCs, which increases from the V to U light;
- An increase of EWs after the primary minimum and a decrease of EWs around phase 0.9;
- A variable activity of the system;
- A mid-eclipse brightening (or brightness variations) in the secondary minimum.

Most of these observational effects can be explained by the mass transfer from the more massive primary to the less massive secondary component and occasional outflow of matter from the system. Both processes can lead to the observed orbital period decrease. The delay of the secondary minimum (largest in U passband) can be explained by the presence of spot(s) on the surface of the contact binary.

The mass loss occurs through the outer Lagrangian point L_2. The density of the escaping gaseous stream, bent by the action of the Coriolis force, quickly decreases (Shu et al., 1979). The observer sees the approach of the most dense parts of the stream just after the primary minimum, which causes an additional decrease of the RV. The gaseous stream causes the equivalent widths of the lines to increase during its projection on the contact system in phases after the primary minimum. Emission from the same stream decreases the equivalent widths of the lines around the phase 0.9. During the large outflow from the system the maximum I is suppressed by absorption in the escaping gaseous stream, so the maximum II is brighter.

The variable activity can be explained in terms of changes of the fill-out factor. When the surface of AW UMa contact binary approaches the outer critical surface (deep LC), the outflow is violent. An uneven distribution of matter in the flow can account for pronounced variations of the LC most marked between the phases 0–0.5.

Streams of matter escaping from the secondary component were also suggested to explain the intrinsic polarization of AW UMa with its maximum around the orbital phase 0.25 (Oschepkov, 1974). This polarimetry was performed from March to May, 1972, close to the periastron passage of the suggested fourth body (the maximum of activity occurred in 1989–90 and P_4 = 17 years). Tidal effects of the fourth body on contact binary could cause an increase of the fill-out factor and outflow of matter from L_2 in 1972. On the other hand, Piirola (1975) did not find any polarization in the light of AW UMa in March and April, 1974.

The mass transfer from the more to less massive component accompanied by mass outflow from the L_2 point, explains the

observed long-term orbital period decrease. It can be shown that both processes get more effective towards the smaller mass ratios.

a) In the case of conservative mass transfer, the relative period change is:

$$\frac{\Delta P}{P} = \frac{3(1-q^2)}{q}\frac{\Delta m}{m}. \quad (11)$$

Observed orbital continuous period decrease of AW UMa can be fully explained by a mass transfer rate Δm = 2.16 10^{-8} $M_\odot$ y^{-1}. If two sudden jumps occurred, the mass required to cause them was Δm = 1.04 10^{-6} $M_\odot$ and Δm = 1.03 10^{-6} $M_\odot$, respectively.

b) If the mass is transferred from the primary to secondary component and afterward lost through L_2 then (Pribulla, 1998):

$$\frac{\Delta P}{P} = \left[\frac{3(1+q)^2}{q}\, r(q)^2 - 3(1+q) + 1\right]\frac{\Delta m}{m}, \quad (12)$$

where $r(q)$ is the distance of the L_2 from the mass center (in the units of the semi-major axis). It is possible to show, that $r(q) \approx 1.2$ for a wide range of mass ratios. To account for an observed period change, the system needs to loose 1.7 times less mass as in the case of the mass transfer (case a). In both formulae, the spin angular momentum of the components was neglected.

Our observations of AW UMa revealed the occasional presence of a mid-eclipse brightening or brightness variability in the secondary minimum. This effect is possibly caused by the matter flowing around the contact system between its surface and the outer critical surface.

The masses of the components of the contact binary (calculated from the mass function $f(m_2)$ = 0.00074 $M_\odot$, inclination angle i = 78.3° and the photometric mass ratio q = 0.08) are M_1 = (1.79±0.14) $M_\odot$ and M_2 = (0.143±0.011) $M_\odot$, so the system is located on the ZAMS. The mean radii of the components are r_1 = (1.87±0.05) $R_\odot$ and r_2 = (0.66±0.02) $R_\odot$. The distance between the components is a = (3.05±0.07) $R_\odot$. The luminosities of the components computed by the W&D code (Sect. 4.2) are L_{1bol} = (7.27±0.39) $L_\odot$ and L_{2bol} = (0.832±0.045) $L_\odot$. The distance to the system calculated from our solution, BC = 0.07, E(B-V) = 0 (Mochnacki, 1981) and $M_{bol\odot}$ = 4.64 is d = (75.9±2.1) pc. This value is somewhat larger than d = (66±4) pc determined by Hipparcos. This discrepancy is probably caused by the presence of other components in the system, which affects the apparent brightness as well as the position of the contact binary on the celestial sphere (see Kovalevski, 1995). Another possible cause of the discrepancy could be the mass outflow from L_2, which increases the amplitude of the RV of the primary component. Agreement with the Hipparcos can be obtained for K_1 = 22.1 km s^{-1}. The corresponding masses of the components (M_1 = 1.20 $M_\odot$, M_2 = 0.096 $M_\odot$) set the system on the TAMS. Further spectroscopic observations in a non-active stage are needed to solve this dilemma.

8.2. Multiplicity of the system

Observational facts relevant for the multiplicity of AW UMa are as follows:

- Changes of the orbital period in the $(O-C)'_2$ diagram (the long-term continuous decrease of the orbital period removed) with a period of P_4 = 6250 days, explained by the light-time effect;
- Changes of the orbital period in the $(O-C)_2$ diagram (the broken-line ephemerides (1)–(3) removed) with a period of 403 days, or in the $(O-C)'_3$ diagram (light-time effect with P_4 = 6250 days removed) with a period of 407 days;
- Systemic velocity variations with a period of 398 days.

The best explanation of the observed changes of the period, systemic velocity and activity involves a quadruple-star model of AW UMa.

The spectroscopic orbit of the mass center of the contact binary with the period P_3 = 398 days provides the mass function $f(m_3)$ = 0.075 $M_\odot$, which can be used to calculate the mass of the third component as M_3 = (0.85±0.13) $M_\odot$, assuming that the orbits of the third component and contact binary are coplanar. The eccentricity of the third component orbit e_3 = 0.227 is rather small, so it is reasonable to assume that the third component evolved together with the contact binary from the same protostellar cloud. The ratio of periods P_3/P_{12}=908 and the almost circular orbit make the triple system highly stable (Kiseleva et al., 1994). The existence of a systemic velocity shifts caused by the third body should be definitely proved by several homogeneous sets of new spectroscopic observations over a 398-day orbital period of the third body.

The possible fourth component revolves around the mass center of the system on a 6250-day-period orbit with eccentricity 0.63. The mass of this component depends on the inclination of its orbit. For inclinations smaller than 30°, the close encounters of this component with the third one would cause the system to be unstable (the ratio of periods is P_4/P_3 = 15.7). For inclinations close to 90°, the fourth component would be too far from the contact binary during the periastron passages to affect its activity. The most probable inclinations of the fourth component orbit are $i_4 \sim 60° - 40°$. The corresponding range of its masses is $M_4 \sim 0.168 - 0.229$ $M_\odot$. The orbit of the fourth component, determined from the light-time effect, shows that its last periastron passage occurred in December, 1989. The strongest variations of the LC were recorded in 1989 and 1990 (Derman et al., 1990). In the same time, the surface of the contact binary was close to the outer critical surface (Rucinski, 1992).

Fekel (1992) found in the sample of 3 dozen multiple systems that most of them have orbital periods in the range of 1–20 years. The orbital periods of the third and fourth component of AW UMa are within this range.

If the long period decrease in $(O-C)$ diagram is interpreted as two sudden period changes 6200 days apart, we have to find an internal mechanism connected with the contact system, which triggers the long-term periodicity of the activity. Nevertheless

the quadruple-star model is more elegant than an alternative triple model with an internal activity mechanism.

Acknowledgements. We are indebted to our referee Bruce J. Hrivnak for valuable comments, Karl Gordon for providing us with the two spectra of AW UMa, Karen Witczak and the editor for improvements of English. The work was supported by NATO grant No. 960322 and VEGA grants No. 1282/97 and 5038/98.

References

Allen C.W., 1976, Astrophysical quantities. Athlone Press, London, 208
Bakos G.A., Horák T.B., Tremko J., 1991, BAC 42, 331
Binnedijk L., 1960, Properties of Double Stars. University of Pennsylvania Press, Philadelphia, USA
Demircan O., Derman E., Müyessroğlu Z., 1992, A&A 263, 165
Derman E., Demircan O., Müyesseroğlu Z., 1990, IBVS No. 3540
Duflot M., Figon P., Meyssonnier N., 1995, A&AS 111, 269
Dworak T.Z., Kurpinska M., 1975, Acta Astron. 25, 7
Eaton J.A., 1976, unpublished work (Odessa archive)
Fekel F.C., 1992, In: McAlister H.A., Hartkopf W.I. (eds.) Complementary approach to double and multiple star research. Astron. Soc. Pac. Conf. Ser. 32, 89
Ferland G.J., McMillan R.S., 1976, IBVS No. 1176
Grygar J., Cooper M.L., Jurkevich I., Bull. Astron. Inst. Czechosl., 23, 147
Hart M.K., King K., McNamara B.R., Seaman R.L., Stoke J., 1979, IBVS No. 1701
Heintze J.R.W., In't Zant J.J.M., van't Veer F., 1990, In: Ibanoğlu C. (ed.) Active Close Binaries. Kluwer Academic Publishers, Dordrecht, Holland, 331
Horn J., Kubát J., Harmanec P., et al., 1996, A&A 309, 521
Hrivnak B.J., 1982, ApJ 260, 744
Hrivnak B.J., 1988, ApJ, 335, 319
Irwin J.B., 1959, AJ 64, 149
Istomin L.F., Orlov L.M., Kulagin V.V., 1980, IBVS No. 1802
Kalish M.S., 1965, PASP 77, 36
Kiseleva L.G., Eggleton P.P., Orlov V.V., 1994, MNRAS 270, 936
Kovalevsky J., 1995, Modern Astrometry. Springer Verlag, Berlin, 225
Kudzej I., 1987, In: Harmanec P. (ed.) Astrophysics. Publ. Astron. Inst. Czechosl. Acad. Sci., Prague, No. 70, 325
Kurpinska-Winiarska M., 1980, IBVS No. 1843
Kwee K.K., van Woerden H., 1956, BAN 12, 327
Liu Q., Yang Y., Zhang Y., Wang B., 1990, Chin. Astron. Astrophys. 14, 175
Maceroni C., van't Veer F., 1993, A&A 277, 515
Mauder H., 1972, A&A 17, 1
McLean B.J., 1981, MNRAS 195, 931
McLean B.J., 1983, private communication to Rensing et al. (1985)
Mikolajewska J., Mikolajewski M., 1980, IBVS No. 1812
Mochnacki S.W., 1981, ApJ 245, 650
Mochnacki S.W., Doughty N.A., 1972, MNRAS 156, 51
Müyesseroğlu Z., Gürol B., Selam S.O., 1996, IBVS No. 4380
Oprecsu G., 1997, private comunication
Oschepkov V.A., 1974, IBVS No. 884
Paczynski B., 1964, AJ 69, 124
Piirola V., 1975, IBVS No. 1060
Pribulla T., Chochol D., Rovithis-Livaniou H., Rovithis P., 1997, IBVS No. 4435
Pribulla T., 1998, Contrib. Astron. Obs. Skalnaté Pleso 28, 101
Rensing M.J., Mochnacki S.W., Bolton C.T., 1985, AJ 90, 767
Rucinski S.M., 1973, Acta Astron. 23, 79
Rucinski S.M., Brunt C.C., Pringle J.E., 1984, MNRAS 208, 309
Rucinski S.M., 1992, AJ 104, 1968
Shu F.H., Lubow S.H., L. Anderson, 1979, ApJ 229, 223
Srivastava R.K., Padalia T.D., 1986, Ap&SS 120, 121
Wilson R.E., Biermann P., 1976, A&A 48, 349
Wilson R.E., Devinney E.J., 1971, ApJ 166, 605
Wilson R.E., Devinney E.J., 1973, ApJ 182, 539
Woodward E.J., Koch R.H., Eisenhardt P.R., 1980, AJ 85, 50
Yim J.R., Jeong J.H., 1995, Kor. J. Astron. Space Sci. 12, 44